Blind source separation methods used in functional brain imaging

Zoltán Géza Tóth

Obuda University Kandó Kálmán Faculty of Electrical Engineering

Institute of Electronics and Communication Systems

Department of Telecommunication

1084, Budapest

Tavaszmező utca 15-17.

toth.zoltan@kvk.uni-obuda.hu

Summary – In my presentation, I will introduce the data analysis methods used in functional brain imaging. I will review the pre-processing steps used to improve the signal-to-noise ratio. I will describe the basics of blind source separation (BSS) methods—independent component analysis (ICA) and extended spatial decorrelation (ESD)—and how these methods can be applied in modern functional brain imaging, such as optical imaging of internal (within human body) signals or functional magnetic resonance imaging.

1 Introduction

In my previous work, I presented the physiological knowledge related to my research and described the structure of the completed laboratory. I assume that the reader has read my previous work before reading this material, so I will not repeat the terms I explained in that paper.

In this document, I will discuss the processing of measured image data. As a first step, I will describe the data structure of the video files obtained during the measurement series and their pre-processing.

In order to understand the detailed analysis following the pre-processing, I will review the various BSS methods, with focusing on their advantages and disadvantages. I present the initial results of my research through a few examples.

2 Image data structure and pre-processing

The amount of data recorded during a trial depends on the ROI. Each trial has a raw file that stores the 12-bit camera signal in 16 bits (MATLAB cannot handle 12-bit variables). The size of these raw files usually exceeds 100 MB (a 500 x 500 pixel, 10-second video file at a camera speed of 28 frames per second is 500 x 500 x 10 x 28 x 2 = 140,000,000 bytes, i.e. 133.5 MB). An experiment usually consists of 30 trials, which means a total data volume of over 3 GB. A complete series of experiments requires approximately 200-300 GB of storage capacity. It can be concluded from the above that the files recorded during the measurements require pre-processing, which reduces their size.

Pre-processing is also necessary because the useful information content of these files is less than 0.1 per cent. This is because physiological artefacts (heartbeat, breathing and 0.1 Hz V signal) cause an order of magnitude greater haemodynamic changes than the component to be examined. [1]

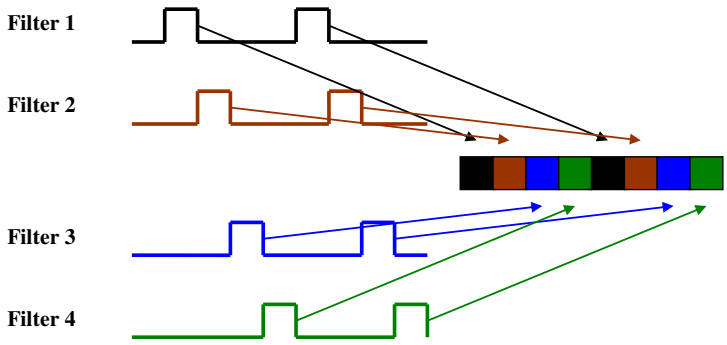

Figure 1. The temporal nature of individual light sources and the location of the corresponding images in the raw file.

Figure 1 illustrates the position of different monochrome illuminated images within the raw file. The first step in pre-processing is to separate the individual monochrome components and average them into trials. This results in four MATLAB files of approximately 100 MB each. Using a camera with a speed of 28 images per second, each filter will have 7 images per second. Calculated with a trial length of 11 seconds, this will result in 77 images per filter.

In the next step, the data for each full second is averaged per filter, which reduces their size by a further seventh. The averaged data per second is called a bin, and the process itself is called binning. Thus, at the end of the binning process, 4x11 bins are created. The final step of pre-processing is called first frame analysis, which essentially involves extracting the image before stimulation (first second) from the other images, so that the resulting bin, which is now one less, will

contain difference signals that make it easier to track the changes we are looking for. As shown in Figure 2, at the end of the process, we obtain 10 difference images averaged over 1 second per filter.

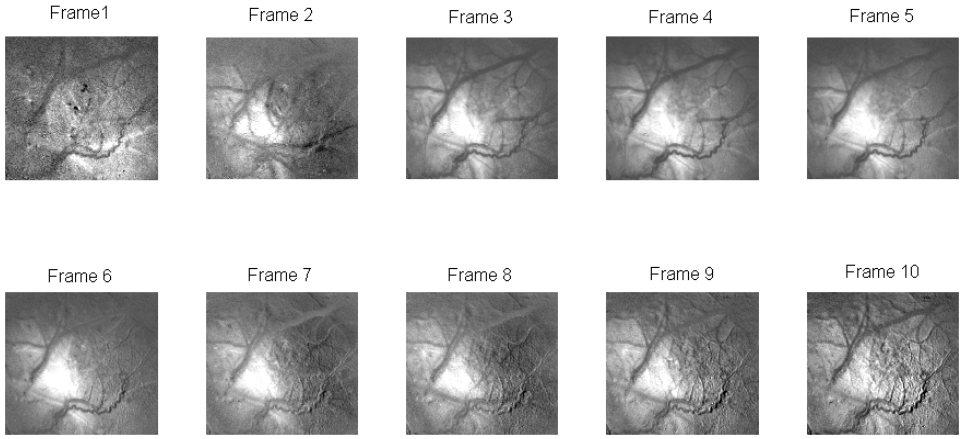

Figure 2 Difference images averaged per second with a 577 nm filter. Here, the appearance and subsequent fading of the activated area is clearly visible.

Before describing the further processing steps, I will present the related mathematical background.

3 BSS procedures

To understand BSS procedures, the cocktail party problem shown in Figure 3 is often cited as an example. Given the recorded signals $x_1(t)$ and x2(t), only a special statistical procedure (BSS) can be used to reproduce the original sources (s1(t), s2(t)) with high accuracy.

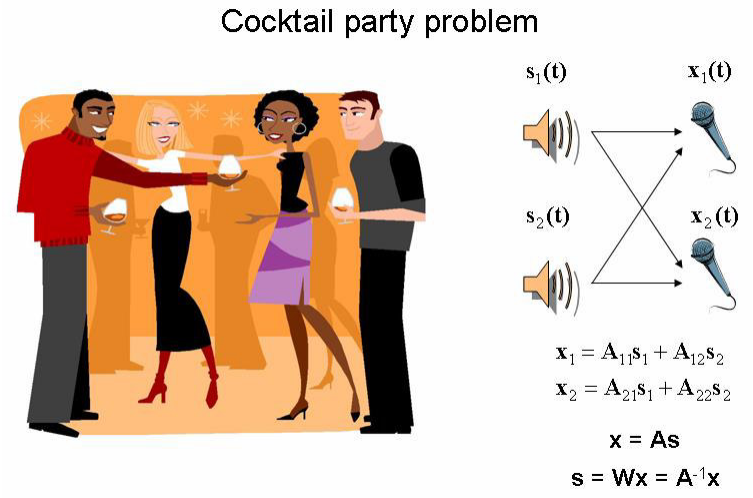

Figure 3. The cocktail party problem. Two talking partners are the two signal sources, s1(t) and s2(t), or s in vector form. Two microphones record the data, x1(t) and x2(t), or x in vector form. In this case, x will be a mixture of s, x=As, where A is unknown, so the original sources cannot be reproduced directly from the recorded signal without a special statistical procedure.

3.1 Principal Component Analysis:

Principal component analysis (PCA) is commonly used to find the original source vector. PCA is now part of major statistical software packages such as SPSS. This procedure can calculate a set of signals from the recorded data that are statistically uncorrelated. In other words, the PCA procedure searches for a linear transformation matrix that can be used to determine the elements of the signal set with the greatest variance or standard deviation. [2] However, in some cases, uncorrelatedness is not a sufficient condition. Figure 4 shows a two-variable joint distribution that is not orthogonal. In this case, only the ICA method can correctly determine the eigenvalues and eigenvectors.

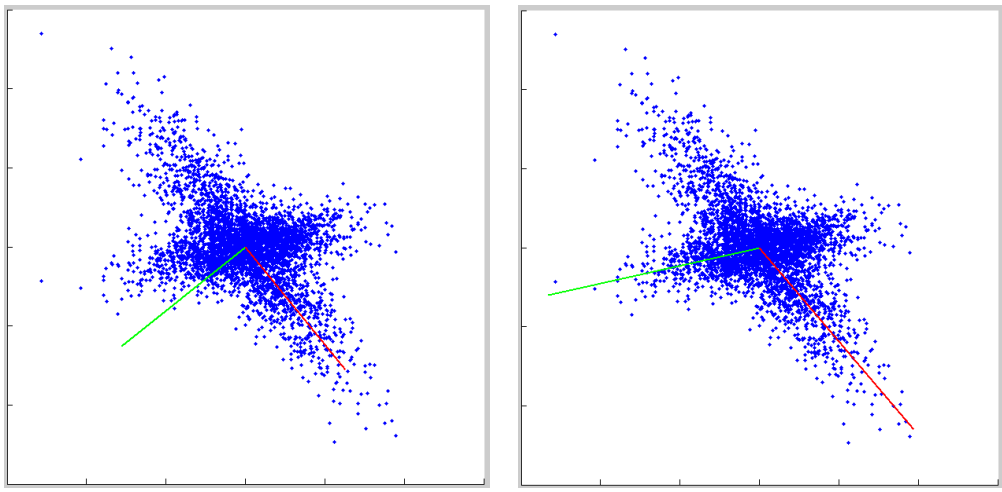

Figure 4 PCA cannot calculate the correct eigenvalues and eigenvectors because the joint distribution of the data is not orthogonal. The figure on the left shows the result of the PCA method. PCA correctly determines the first principal component (red line), but incorrectly calculates the second component (green line). In contrast, the components determined by ICA, shown in the figure on the right, are correct

However, PCA is also a useful tool in this case, because it can be used to transform the data set into a coordinate system in which the direction of one of the basis vectors is given by the first eigenvector. PCA can therefore be used as a pre-processing method for independent component analysis (ICA). [1][3][4]

3.2 Independent component analysis:

The goal of ICA is to determine the inverse mixing matrix $\mathbf{W} = \mathbf{A}^{-1}$. With the help of this matrix, the independent sources $\mathbf{s'=Wx}$ can then be restored with high accuracy from their noisy mixture. If the noise can be ignored, the inverse mixing matrix can be written in the following form: $\mathbf{W=\Lambda PA}^{-1}$, where P is a permutation matrix and $\mathbf{\Lambda}$ is a diagonal matrix containing the unknown variances of the sources. [4][5][6]

Sphering is the name given to the pre-processing step in which the data set is transformed into a new coordinate system using the PCA method. This greatly simplifies the determination of the inverse mixing matrix. This procedure transforms the data set so that the components obtained have a mean of zero and a covariance of unity. [1][5][7]

The independence of the components can be determined by their deviation from the Gaussian distribution. Assuming that the source signals are not normally distributed, which is true for random signals, the distribution of their mixture is

more normal than the distribution of any of the original signals (central limit theorem), so it is sufficient to find the inverse mixing matrix for which the recovered sources are most non-normally distributed. The various ICA methods are basically based on the following two algorithms:

- Infomax. This method is based on determining the entropy of the data set, since a probability variable that deviates more from the normal distribution has greater entropy and greater information content. Negentropy, the deviation from the entropy of a normally distributed variable, is often used, as its value is zero for normal distribution and otherwise a non-negative number. This method is therefore based on finding the maximum negentropy. Thus, it is sufficient to find the inverse mixing matrix for which the recovered sources are most non-normally distributed. The various ICA methods are basically based on the following two algorithms:
- Maximising kurtosis. Kurtosis can be calculated from the second and fourth moments of the probability variable. Its value is zero in the case of a normal distribution. If the kurtosis is negative, the distribution is called sub-Gaussian; if it is positive, it is called super-Gaussian. The distribution function of super-Gaussian signals is more peaked in the middle and has 'heavier tails' at the edges than the distribution function of normally distributed variables.

There are conditions for using ICA, and unfortunately, there are also disadvantages:

- Only one of the original source signals could have a normal distribution.
- The number of the original source signals must be less than or equal to the number of measured signals.
- ICA is a computationally intensive and slow process. The so-called FastICA algorithms, developed to increase speed, do not calculate kurtosis, but use approximation functions instead.
- The order of the results obtained is unknown, so the individual independent components can only be identified by some special attributes.
- As a result of sphering, the average of the independent components is also zero and their covariance is unity, i.e. the expected range of the component amplitude must be known for rescaling. Figure 5 shows an example of this. If we know that the source variables are wav files, then the resulting components can be rescaled to a value between ±1 which is typical for wav files, otherwise rescaling cannot be performed.

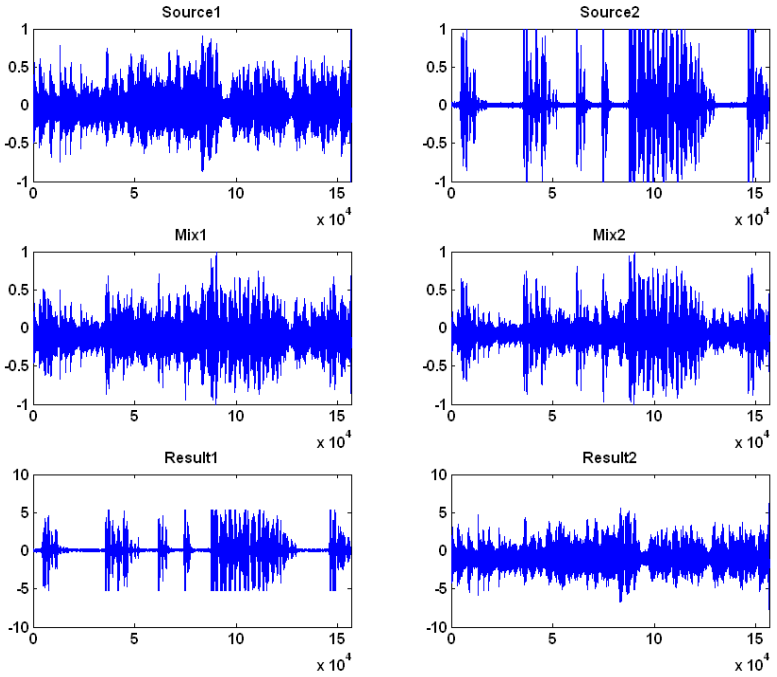

Figure 5 Mix1 and Mix2 are two wav files, a mixture of Source1 and Source2. The two components restored with ICA are Result1 and Result2.

3.3 Extended Spatial Decorrelation:

Molgedey and Schuster developed another possible method for determining independent signals. They called their method timed delay decorrelation. The essence of this method is that it delays a signal with a zero mean value and unit variance (if the signal is not like this, it must be transformed first). The delayed signal is analysed, and the resulting transformation procedure is then applied to the undelayed signal. This procedure requires much less computation and therefore takes much less time than the ICA procedure. [8]

A German research group modified this procedure to allow image signals to be analysed. The procedure was named extended spatial decorrelation (ESD). Instead of creating a new data series with a time shift, the additional image series is created by shifting the images horizontally and vertically. [1][7]

The following conditions must be met in order to use the ESD method:

- The spatial distribution of the original sources must be uniform.
- Among the original sources, the covariance must be zero, i.e. the sources must be uncorrelated.

- The original source and its spatially shifted version must also be uncorrelated.
- The autocovariance of each source must be different.

According to Schiessl, the ESD method is sufficiently robust to calculate independent components even if their sources are slightly dependent on each other and their variation is very small (<0.1%). [1][9]

3.4 Application of BSS algorithms:

ICA was originally developed for analysing neuroscience data, such as EEG, but today it is increasingly used in other areas of life. Examples of such applications include:

- Analysing economic data and finding hidden correlations within it.
- Image noise filtering.
- In telecommunications, for example in mobile communications, separating one's own signal from the signals of other users causing interference using Code-Division Multiple Access (CDMA).

However, the ICA method is still most commonly used today for analysing neurological data. Following this theoretical overview, I will return to describing the processing of my own measured results.

4. Further analysis of the pre-processed data

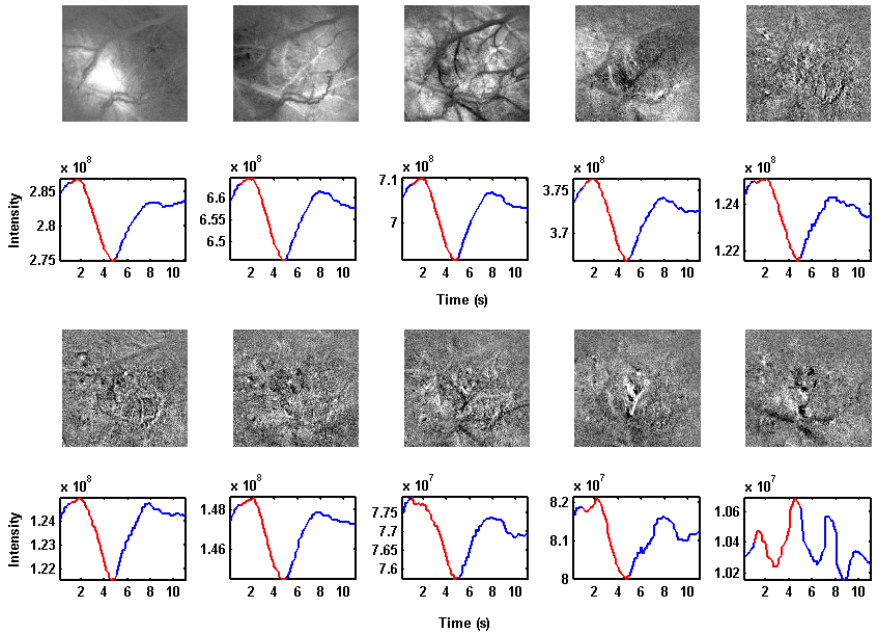

Figure 6. Independent image components calculated from difference signals and their temporal changes. The first image shows the active area, the next two images show the veins and arteries, while the others essentially contain only noise. On the time functions, the part drawn in red shows the time of stimulation.

To generate spatially independent components, the 10 difference image signals calculated earlier must be analysed based on their spatiality rather than their temporality. This means that the image elements that make up each image must be sequentially concatenated, and the resulting vectors, whose number will correspond to the number of bins, must be considered as a measured element. It follows from the above that this method can be used to produce a number of independent image components equal to the number of bins. Figure 6 shows the independent image components of the difference signals previously shown in Figure 2. Let the values of the frames averaged over the original trials, decomposed into column vectors, form the S matrix. The number of elements in the column vectors is x·y, where x and y are the number of rows and columns in the image. Let the value of the current independent image component decomposed into row vectors be r, whose number of elements is also x·y. Below each component, you can see its time domain evolution, which I calculated using the r·S product.

The time domain behaviour can be further refined if the calculation is performed not on the entire image, but only on its activated area. Figure 7 shows the GUI I developed, where, in addition to the ESD component showing the activated area for each filter, only the time domain signal calculated for a small part of the activated area is visible.

Figure 7 shows that the signals obtained in the time domain (especially the 700 nm component) are noisy. Further improvement in the signal-to-noise ratio can be achieved by averaging the signals obtained in the time domain using the above method over several series of experiments. Of course, averaging can only be performed on the same stimulated whisker and the same stimulating signal shape. Figure 8 shows the time domain signals averaged per whisker and per signal shape for a series of experiments performed on several subjects under different lighting conditions. The figure clearly shows that in the case of sinusoidal stimulation, the response is much noisier, with oscillation in some cases. This was to be expected, as the energy content of a square wave signal with the same amplitude is greater. Approached from another angle, the harmonic content of the square wave causes a stronger haemodynamic response (recall the logarithmic relationship between spike frequency and stimulation frequency described in the previous document).

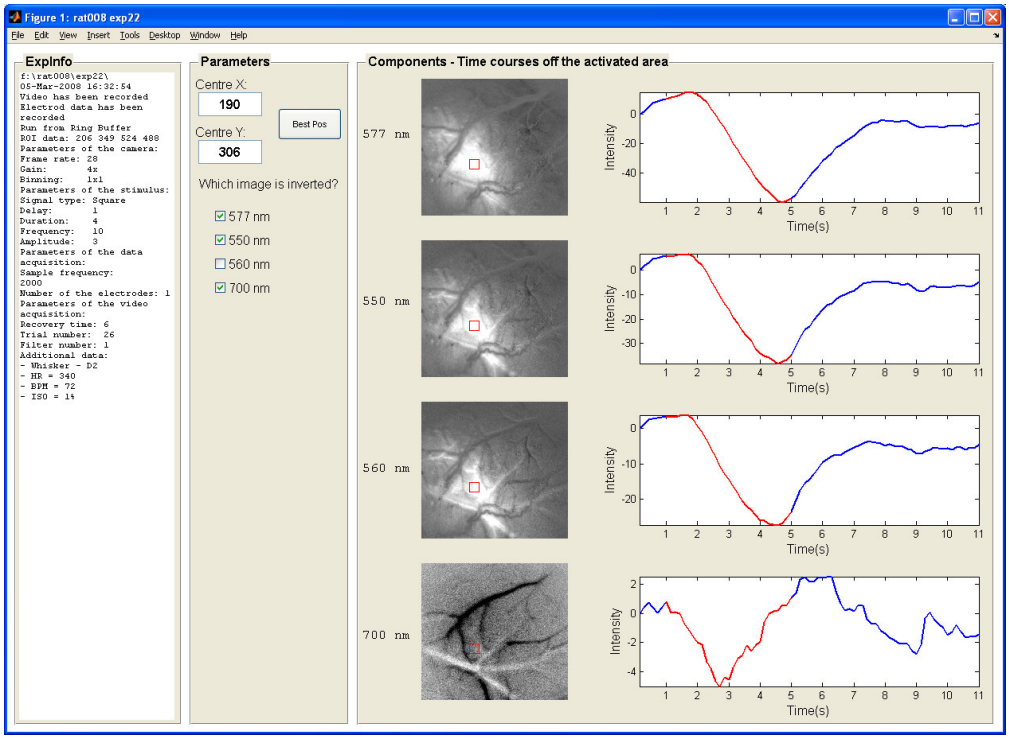

Figure 7 GUI shows the activated areas for an experiment. The box on the left side of the GUI shows the parameters of the experiment. In the Parameters panel, you can set which part of the active area the

programme should use to calculate the signal in the time range. The selected area is marked with a small red square. The position of the square can also be adjusted by clicking on the top image (577 nm). As I mentioned earlier, the ESD component is not scaled, so it may happen that the ESD calculates an inverted image (the black and white areas are swapped). The images can therefore be inverted by clicking on the appropriate checkbox.

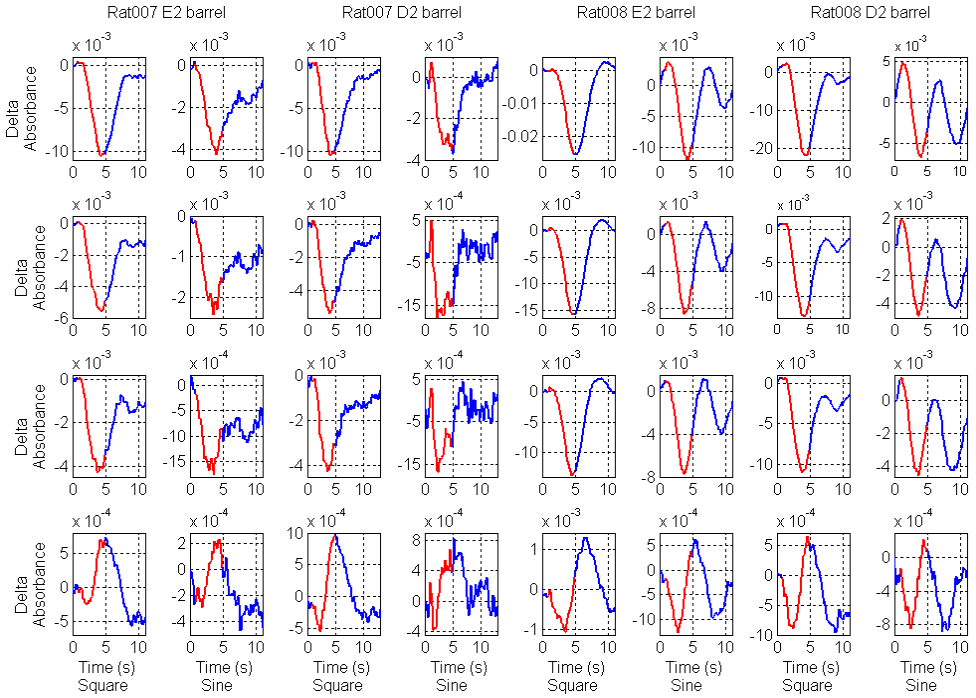

Figure 8 Signal shapes averaged over time ranges per subject, per stimulated moustache and per stimulus signal shape. The vertical axes of the figures show the $(I_t-I_0)/I_0$ delta absorbance value, where I_0 is the intensity value obtained at t=0 and I_t is the intensity value obtained at time t.

Summary

The results of the analyses performed so far are consistent with the results of previous studies. [10][11] I drew Figure 9 to verify the calculation of the activated areas. When stimulating different moustaches, the activated areas coincide with the barrels obtained by tissue staining.

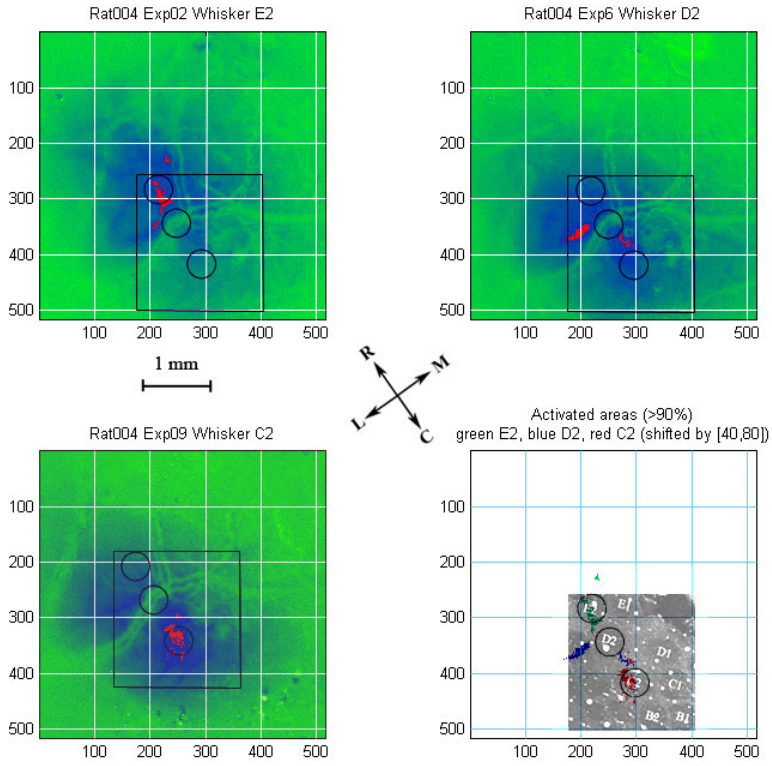

Figure 9. In the first three figures, the areas highlighted in red indicate the activated part (areas with an intensity exceeding 90%). In the second image, the activated areas drawn on the stained section almost coincide with the barrels highlighted with black circles. The results of histology (tissue staining) are indicated by black outlines in the other three images. The position of the image corresponding to the C2 moustache differs from the others because the camera moved. The degree of displacement is [40.80] pixels, which I calculated based on a well-defined point (the junction of the blood vessels).

The data in this document contains twenty series of measurements. In the calculations performed so far, I have only analysed the response to individual light components, which only gives a rough approximation of the changes in the main physiological characteristics described in the previous document. This analysis therefore needs to be refined further by calculating the components corresponding to the actual physiological processes from the recorded spectral data and then analysing the data obtained in the manner outlined above.

Acknowledgement

I would like to take this opportunity to thank Dr. Zsolt Temesvári, György Molnár, Dr. Tibor Wührl and Ildikó Grega for organising this conference, my supervisor Dr. Ingo Schiessl and my advisor Dr. John Gigg for their help at the

University of Manchester, the head of OE KVK EKRI, Dr. Péter Varga, for the support received from the Institute, the UK Biotechnology and Biological Sciences Research Council (BBSRC) for the three-year scholarship they awarded me.

Last but not least, I would like to express my special thanks to my wife, Dr. Gabriella Juhász, for her help in understanding the physiological parts, and to my family for putting up with my keyboarding late into the night.

References

[1] Schiessl, I., Stetter, M., Mayhew, J. E., McLoughlin, N., Lund, J. S., and Obermayer, K. (). "Blind signal separation from optical imaging recordings with extended spatial decorrelation." *IEEE Trans Biomed Eng*, 47(5), 573-7. 2000

[2] Stone, J. V. Independent Component Analysis: A Tutorial Introduction, *London: Bradford Book.* 2004

[3] Hyvarinen, A. Independent Component Analysis: A Tutorial [internet] (Updated April 1999) Available at: http://cis.legacy.ics.tkk.fi/aapo/papers/IJCNN99_tutorialweb/IJCNN99_tutorial3.html [accessed 10 October 2025] 2000

[4] Hyvarinen, A., Karhunen, J., and Oja, E. Independent Component Analysis, *New York: John Wiley & Sons Inc.* 2001

[5] Comon, P. "Independent component analysis, A new concept?" *Signal Processing*, 36, 287-314. 1992

[6] Hyvarinen, A. "Fast and robust fixed-point algorithms for independent component analysis." *IEEE Trans Neural Netw,* 10(3), 626-34. 1999

[7] Stetter, M., Schiessl, I., Otto, T., Sengpiel, F., Hubener, M., Bonhoeffer, T., and Obermayer, K. "Principal component analysis and blind separation of sources for optical imaging of intrinsic signals." *Neuroimage*, 11(5 Pt 1), 482-90. 2000

[8] Molgedey, L., and Schuster, H. G. "Separation of a mixture of independent signals using time delayed correlations." *Phys Rev Lett,* 72(23), 3634-3637. 1994

[9] Schiessl, I. Blind Source Separation Algorithms for the Analysis of Optical Imaging Experiments, *Technischen Universität Berlin*, Berlin. 2001

[10] Nemoto, M., Nomura, Y., Sato, C., Tamura, M., Houkin, K., Koyanagi, I., and Abe, H. "Analysis of optical signals evoked by peripheral nerve stimulation in rat somatosensory cortex: dynamic changes in hemoglobin concentration and oxygenation." *J Cereb Blood Flow Metab*, 19(3), 246-59. 1999

[11] Sheth, S. A., Nemoto, M., Guiou, M. W., Walker, M. A., and Toga, A. W. "Spatiotemporal evolution of functional hemodynamic changes and their relationship to neuronal activity." *J Cereb Blood Flow Metab*, 25(7), 830-41. 2005